Testing Energy Balance Climate Models

JAMES A. COAKLEY, JR., AND BRUCE A. WIELICKI

National Center for Atmospheric Research[1], Boulder, CO 80307

(Manuscript received 29 June 1979)

Adopting procedures often applied to model the earth's climate, we use zonal fields from the control run of a general circulation climate model (GCM) (Wetherald and Manabe, 1975) to construct parameterizations of the energy budget components for use in a simple Budyko-Sellers energy balance climate model (EBM) (North, 1975). Comparing the results of the GCM and the EBM for changes in solar constant, we find that with these parameterizations changes in the surface temperature calculated with the EBM are substantially larger than those calculated with the GCM. Furthermore, when the meridional energy transport in the EBM is held constant so that it simulates the transport in the GCM, the results of the two models diverge hopelessly. On the other hand, with the parameterizations of the EBM modified to simulate the behavior of the GCM fields, the results of the two models agree fairly well. This exercise illustrates the weakness of current methods used to extract parameterizations for EBMs from observations of the present climate.

1. Introduction

Many have used the simple models introduced by Budyko (1969) and Sellers (1969) to study the earth's climate and its sensitivity to various perturbations. These models are based on the conservation of energy. Each component taking part in the energy balance is parameterized to be a simple function of surface temperature and latitude. In mean annual models the zonal average surface temperature for a particular latitude belt is obtained by balancing the fluxes of infrared emission and net meridional transport out of the belt with the flux of solar radiation absorbed by the belt. Of course, such models give a highly simplified picture of the climate system and whether they give results that are representative of the system is open to question. In this paper we suggest one possible method of assessing the validity of such models.

Our suggestion is to compare the results of the models with those of more sophisticated models such as, for example, three-dimensional numerical general circulation climate models (GCMs). Like the climate system, GCMs include many physical processes, e.g., evaporation, precipitation, convection, . . . , that are either ignored or crudely parameterized in EBMs. Of course, the processes included in GCMs are often simple representations of those that influence the climate. Furthermore, of the processes that influence the climate, few have been incorporated into models. Consequently, we do not expect GCMs to predict the behavior of the climate system. Nevertheless, because they include a multitude of physical processes, GCMs, like the climate system, have many more degrees of freedom than do the EBMs. These degrees of freedom can give rise to feedbacks that affect the results obtained with the model. The question is whether, despite such feedbacks, EBMs can model the behavior of the system. If EBMs cannot model the behavior of GCMs, we would be astonished if they could model the behavior of the climate.

Typically, parameterizations used in EBMs are derived from observation of the present climate and they are usually designed so that the model recovers the observed temperatures and energy fluxes. Using the results of a GCM as observational data, we may apply procedures commonly used for modeling the earth's climate to develop parameterizations for an EBM that is to simulate the behavior of the GCM. Once the parameterizations are developed, we can test the EBM to see if it responds to changes like the GCM. In this manner we test the methods of parameterization adopted for the earth. The GCM results used in this paper are from the solar constant change experiments performed by Wetherald and Manabe (1975).

2. An EBM to model the GCM

To model the behavior of the GCM we adopt North's (1975) EBM. This model is simple and North has demonstrated its equivalence to the earlier Budyko and Sellers models. The condition of energy balance is given by

[1] The National Center for Atmospheric Research is sponsored by the National Science Foundation.

0022-4928/79/112031-09$06.25

TABLE 1. Legendre mode amplitudes for GCM fields.

Experiment solar constant change	n	Absorbed solar radiation (W m^{-2})	rms error	Emitted thermal radiation (W m^{-2})	rms error	Surface temperature (°C)	rms error
+2%	0	240.8	67.61	238.0	24.04	26.91	14.66
	2	−150.2	7.89	−52.0	6.07	−32.12	2.93
	4	−21.5	3.31	−13.9	3.94	−7.15	1.70
0%	0	234.4	67.91	231.7	25.36	23.93	15.94
	2	−150.6	8.72	−55.0	6.17	−34.82	3.39
	4	−24.4	3.18	−13.8	4.11	−7.39	2.34
−2%	0	226.8	70.14	224.4	27.03	19.52	17.58
	2	−155.2	9.97	−58.9	6.14	−38.39	3.78
	4	−28.8	2.67	−15.6	3.28	−9.73	1.94
−4%	0	217.4	73.53	215.1	30.14	13.82	19.91
	2	−162.7	10.60	−66.0	6.15	−43.93	3.24
	4	−27.7	5.22	−14.5	3.81	−8.52	1.56

$$-D\frac{d}{dx}(1-x^2)\frac{d}{dx}T(x) = QS(x)[1-\alpha(x,x_s)] - F[x,T(x)], \quad (1)$$

where D is a constant; $T(x)$ is the surface temperature at latitude θ; $x = \sin\theta$; Q is the solar constant divided by 4 (as in the GCM experiments to be modeled, $Q = 348.8$ W m^{-2}); $S(x)$ is the fraction of Q incident at x; $\alpha(x,x_s)$ is the albedo at x when the snow line, which is described below, is at x_s; and $F[x,T(x)]$ is the flux of emitted thermal radiation. The term on the left-hand side of (1) represents the divergence of the flux of energy transported across the latitude designated by x. This is balanced by the net radiative flux at x given by the two terms on the right-hand side. With the albedo and emitted thermal radiation parameterized to be simple functions of surface temperature, we can readily obtain the solution to (1) by using a series of Legendre polynomials to represent each of the fields (North, 1975). These fields are thus represented by

$$Z(x) = \Sigma_n Z_n P_n(x), \quad (2)$$

where Z_n is the amplitude of the nth mode and $P_n(x)$ the Legendre polynomial of order n. With such expansions, (1) becomes a set of algebraic equations to be solved for the amplitudes of the surface temperature.

Listed in Table 1 are the amplitudes of the GCM's surface temperature, absorbed solar radiative flux and emitted IR radiative flux for the four solar constant change experiments performed by Wetherald and Manabe (1975). Because the GCM's Northern and Southern Hemispheres are identical, the amplitudes of the modes with odd n are zero. The rms error listed with the amplitudes is the rms deviation of the series, which is truncated at the designated term, from the GCM's field. As with the earth the errors are small for $n \geq 2$ (North, 1975; North and Coakley, 1979).[2]

To parameterize the albedo, we adopt North's model

$$\alpha = \begin{cases} \alpha_0 + \alpha_2 P_2(x), & x < x_s \\ \beta_0, & x > x_s, \end{cases} \quad (3)$$

where β_0 is set equal to the mean albedo of snow and ice covered regions and where α_0 and α_2 are adjusted to retrieve the $n = 0$ and $n = 2$ amplitudes of the solar radiative flux absorbed in the GCM's control experiment (0% solar constant change). Choosing the snow line x_s to be at the −4°C isotherm of the surface temperature, we obtain $\beta_0 = 0.59$, $\alpha_0 = 0.33$ and $\alpha_2 = 0.095$. The −4°C isotherm coincides with the accumulation of snow in the GCM.

For IR emission we use the latitudinal variation of the GCM's zonal average surface temperature and IR flux to obtain a relationship between the two. As for the earth (Cess, 1976), the emitted flux for the GCM is well approximated by

$$F(x,T) = A_1 + B_1 T(x) + A_2 A_c(x), \quad (4)$$

where A_1, A_2 and B_1 are constants and $A_c(x)$ is the fraction of cloud cover in the model. Cess (1976) found that $A_1 = 257$ W m^{-2}, $B_1 = 1.63$ W m^{-2} °C^{-1} and $A_2 = -91$ W m^{-2} gave the best fit to observations for the earth's Northern Hemisphere. We find that $A_1 = 236.9$ W m^{-2}, $B_1 = 1.28$ W m^{-2} °C^{-1} and $A_2 = -71.1$ W m^{-2} give the best fit to the GCM fields for the control experiment. The fluxes obtained with (4) are compared with those of the GCM in Table 2. As with the earth, the errors obtained with (4) are generally less than 1%. The 2% errors shown in Table 2 occurs where the top layer of clouds in the GCM jumps from one vertical grid point to the next. The jump in cloud height causes a sudden change in the variation of the emitted flux with latitude that is impossible to capture with (4).

To complete the parameterizations, the diffusion coefficient D is set to 0.457 W m^{-2} °C^{-1} so that T_2 calculated with the EBM equals that of the GCM for the control experiment.

With the parameterizations developed in this fashion, the first two modes of the surface temperature obtained with the EBM are guaranteed to agree with those obtained with the GCM for the control

[2] As is indicated by the amplitudes in Table 1, for global average conditions ($n = 0$) the GCM absorbed more energy than it emitted. Following Dickinson (private communication), we presume that this extra energy, which is only 1% of the absorbed solar radiative flux, would have been dissipated by friction that is included in the model's momentum equations but not explicitly in the model's thermodynamic equation. In the EBM, we allow for this additional energy by setting the $n = 0$ component of the meridional transport equal to the global average net radiative flux of the GCM control experiment (0% solar constant change).

experiment. We now perform the solar constant change experiment to see whether the EBM behaves like the GCM. To judge the success of the EBM, we compare the changes ΔT_0 calculated for the global average surface temperature and the feedbacks $\Delta F_0/\Delta T_0$ and $Q\Delta\alpha_0/\Delta T_0$. The change in the global average surface temperature for a given change in solar constant is a measure of the model's sensitivity, while the feedbacks govern this sensitivity. We obtain a relationship between these quantities from the condition of global energy balance,

$$F_0 = Q[1 - \alpha_0(x_s)], \tag{5}$$

where

$$\alpha_0(x_s) = \int_0^1 dx S(x)\alpha(x,x_s).$$

Differentiating (5) we obtain

$$\frac{dT_0}{dQ} = \frac{(1 - \alpha_0)}{dF_0/dT_0 + Qd\alpha_0/dT_0}. \tag{6}$$

The results for the GCM are listed in Table 3, those for the EBM in Table 4. The EBM proves to be more sensitive than the GCM to changes in the solar constant. Considering the simplicity of the EBM, the differences might seem small. We should recognize, however, that the smallness of the differences is due to the cancellation of competing factors. For example, the albedo-temperature feedback in the EBM is smaller than it would have been had the meridional transport in the model behaved like that in the GCM. The diffusive model used to calculate the meridional transport of heat in the EBM inhibits cooling at polar latitudes, thereby inhibiting the equatorward advance of snow cover. In the GCM, on the other hand, the poleward transport is the net of two components, the transport of dry static energy and the transport of latent energy. As the solar constant changes, sizeable changes take place in both components, but for the range of solar constants under consideration, changes in the transport of dry static energy nearly compensate changes in the transport of latent energy (Wetherald and Manabe, 1975). As a result, the total meridional transport remains relatively constant despite increases in the model's pole-to-equator surface temperature gradient. In Fig. 1 the divergence of the GCM's transport is compared with that obtained by using the diffusive model. With constant transport, the albedo-temperature feedback in the EBM would be stronger and the model would be even more sensitive than is indicated in Table 4.

With the transport in the EBM set to be constant and equal to that in the GCM, however, the surface temperatures of the GCM control experiment no longer represent a stable climate in the EBM. Instead, the EBM produces three stable climates for a 0% solar constant change: one free of ice and snow and having a surface temperature of 19.0°C, one with the snow line 17° equatorward of its position in the control experiment and having a surface temperature of 18.3°C, and one with the snowline at the equator.

Clearly, an EBM designed in this fashion fails to model the behavior of the GCM. Even though the parameterizations used in the EBM fit the climatic state produced with the GCM, they fail to model the changes that took place. Parameterizations developed in a similar fashion for the earth could obviously exhibit the same deficiency. Unlike parameterizations for the earth, however, parameterizations might be constructed so that they produce

TABLE 2. GCM grid-point values of emitted IR flux for control experiment and IR flux computed using (4) along with surface temperatures and cloud amounts from control experiment.

GCM grid point	Latitude	Surface temperature (°C)	Cloud amount	IR (W m^{-2})	Calculated IR (W m^{-2})	Error (%)
1	3.00	36.75	0.51	246.6	247.7	0.4
2	8.96	38.15	0.47	252.6	252.3	−0.1
3	14.83	38.38	0.43	256.5	255.5	−0.4
4	20.54	36.99	0.41	254.9	255.1	0.1
5	26.05	33.06	0.41	249.6	250.1	0.2
6	31.31	28.66	0.43	241.7	243.0	0.5
7	36.30	23.58	0.47	229.6	233.7	1.8
8	40.98	18.61	0.52	228.6	223.7	−2.1
9	45.35	15.43	0.57	220.0	216.1	−1.8
10	49.41	12.85	0.60	211.9	210.7	−0.6
11	53.16	10.78	0.63	205.8	205.9	0.1
12	56.61	7.65	0.63	199.7	201.9	1.1
13	59.77	4.40	0.64	196.7	197.0	0.2
14	64.00	0.43	0.63	190.4	192.7	1.2
15	68.79	−8.85	0.63	180.3	180.8	0.3
16	74.43	−13.78	0.62	174.5	175.2	0.4
17	79.72	−27.89	0.59	160.7	159.3	−0.9

TABLE 3. Results for GCM.

Solar constant change	ΔT_0 (°C)	$\Delta F_0/\Delta T_0$ (W m^{-2} °C^{-1})	$Q\Delta\alpha_0/\Delta T_0$ (W m^{-2} °C^{-1})
+2%–0%	2.98	2.1	−0.57
0%–(−2%)	4.41	1.7	−0.67
−2%–(−4%)	5.70	1.6	−0.85

TABLE 4. Results for EBM.

Solar constant change	ΔT_0 (°C)	$\Delta F_0/\Delta T_0$ (W m^{-2} °C^{-1})	$Q\Delta\alpha_0/\Delta T_0$ (W m^{-2} °C^{-1})
+2%–0%	5.90	1.28	−0.44
0%–(−2%)	6.50	1.28	−0.62
−2%–(−4%)	8.16	1.28	−0.71

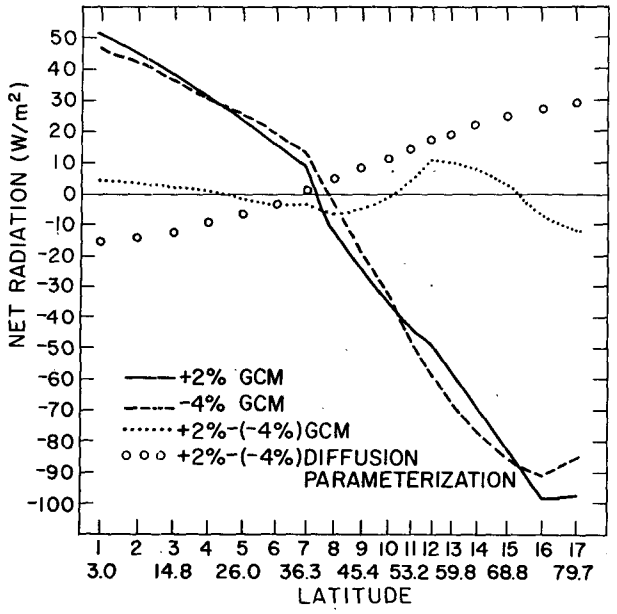

FIG. 1. Net radiation budget (divergence of meridional energy flux) for GCM and for diffusive transport model.

the changes that occurred in the GCM. Such parameterizations are described next.

3. EBM with modified parameterizations

In designing the parameterizations to give the appropriate changes the obvious starting point is the parameterization of the meridional transport. In the GCM this transport remained relatively constant for the range of solar constant changes under consideration. With constant transport $D(x)$ the equation of energy balance becomes

$$D(x) = QS(x)[1 - a(x,T)] - F(x,T). \quad (7)$$

Obviously, this equation may be solved algebraically at each latitude without the Legendre modes used to solve (1). By solving (7) algebraically, however, we find that the condition of energy balance allows several equilibrium states to exist at each latitude. For example, because of the different albedos assigned to snow-free and snow-covered surfaces, one latitude belt may be covered with snow, while on either side its neighbors may be free of snow. To reduce the number of possible solutions, we retain the fourth-order Legendre polynomial representations of the fields. In this way we require a certain degree of smoothness for the latitudinal variation of the solution.

The transport adopted for the EBM is set equal to that in the GCM's control experiment. The mode amplitudes of this transport can be obtained by differencing the mode amplitudes given for the radiation budget components in Table 1.

Turning to the IR flux, the small value of B_1 in (4) clearly forced the sensitivity of the EBM to be much larger than that of the GCM. Furthermore, the small value is not representative of the GCM $\Delta F_0/\Delta T_0$ in Table 3. The failure of the parameterization procedure to produce a representative value of dF/dT is caused in part by the latitudinal variation of cloud heights. The latitudinal variation of cloud heights in the GCM affects the latitudinal variation of the emitted flux and thereby contributes to the value of B_1. As cloud altitude is held constant during the climate change experiments, we should subtract the contribution to B_1 made by changing cloud heights.

To see how cloud height variations affect B_1, we take the flux emitted by the GCM to be given by

$$F = C_1 + \Sigma_i A'_{c_i} C_{2_i}, \quad (8)$$

where C_1 is the flux emitted by regions that are cloud free; C_{2_i} is the difference between fluxes emitted by regions that are completely covered by clouds at level i and those that are cloud free; and A'_{c_i} is the fraction of area covered by clouds at level i but not overlapped by clouds at higher levels (Cess, 1974; Ramanathan, 1977). According to Ramanathan (1977), changes in the flux emitted by the GCM are approximately given by

$$\Delta F = [(\partial C_1/\partial T) + (\partial C_2/\partial T)A_c]\Delta T + (\partial C_2/\partial A_c)\Delta A_c, \quad (9)$$

where $\partial C_2/\partial T = \Sigma_i (A'_{c_i}/A_c)(\partial C_{2_i}/\partial T_{sc_i})(dT_{sc_i}/dT)$; $\partial C_2/\partial A_c = \Sigma_i (\partial A_c/\partial A'_{c_i})^{-1} C_{2_i}$; $T_{sc_i} = T_{c_i} - T$; T_{c_i} is the cloud-top temperature for clouds with tops at level i, and $\partial C_2/\partial T_{sc_i} \approx -1.65$ W m^{-2} °C^{-1} independent of atmospheric profiles of cloud cover, temperature and humidity. By comparing (9) to (4), we recognize that the factor multiplying ΔT in (9) contributes to B_1 and that multiplying ΔA_c contributes to A_2. The term $(\partial C_2/\partial T)A_c$ is the contribution to B_1 due to cloud-height and temperature profile changes. Had the temperature lapse rates in the GCM, in addition to the cloud heights, remained constant, we could subtract the contribution of $(\partial C_2/\partial T)A_c$ to B_1 in order to obtain a better estimate of dF/dT.

The lapse rates in the GCM, however, did not remain constant. In fact, Ramanathan (1977) showed that the changes in $\Delta F_0/\Delta T_0$ were primarily the result of changes in the lapse rates. Using values of dT_{sc_i}/dT and A'_{c_i} from the GCM experiments to compute $(\partial C_2/\partial T)A_c$, we find that lapse rate changes accounted for the latitudinal structure of dF/dT as is shown in Fig. 2.

If in addition to allowing for the latitudinal variation of cloud heights, we could have allowed for changes in the lapse rate, then we could have brought the IR parameterization into agreement with the GCM results. Simple prescriptions for adjusting the lapse rate have been offered by Rennick

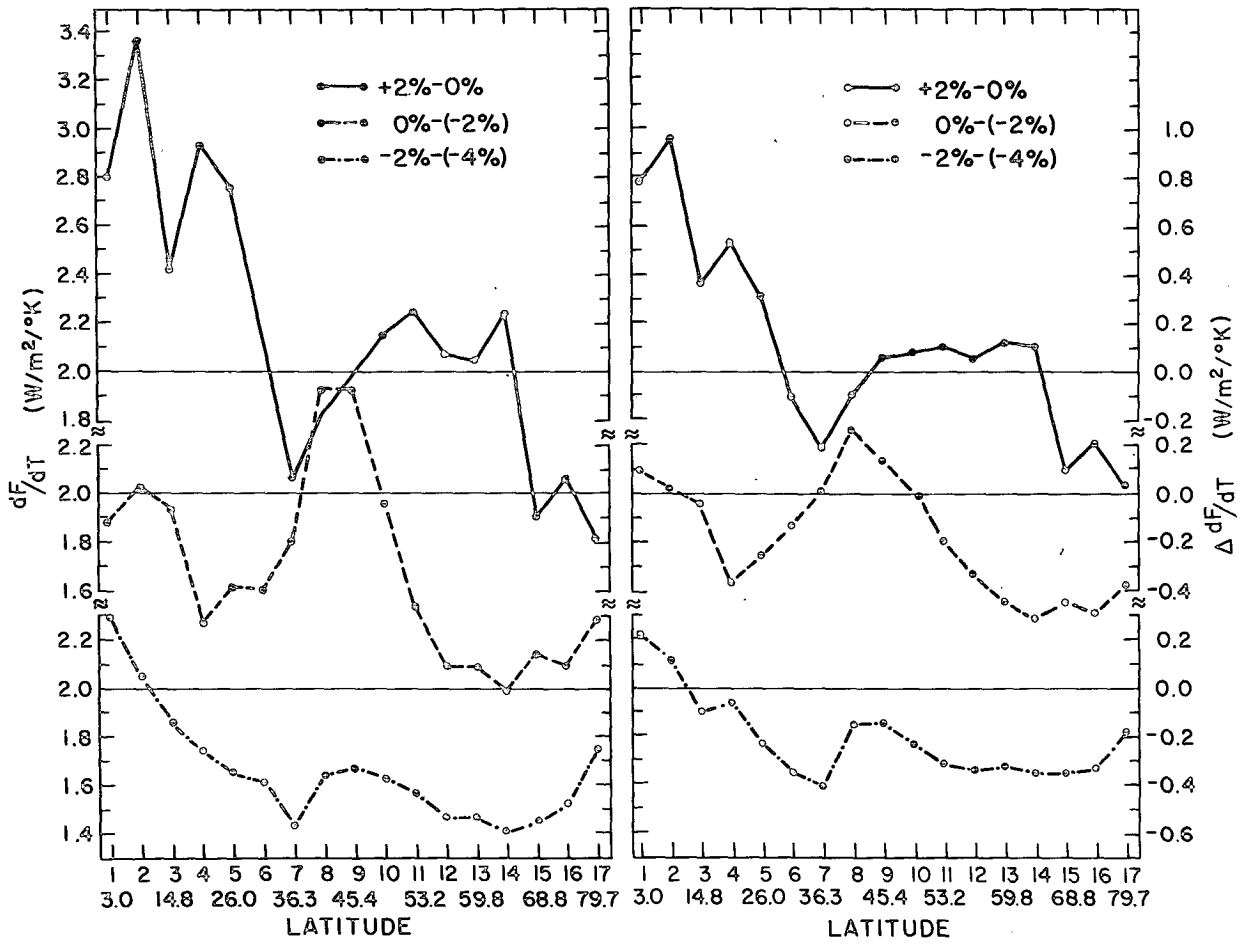

FIG. 2. dF/dT for GCM from the four solar constant change experiments (Wetherald and Manabe, 1975) and $\Delta dF/dT$. $\Delta dF/dT = (\partial C_2/\partial T)A_c$ in Eq. (9).

(1977), by Stone (1978), by Ramanathan and Coakley (1978) and by Stone and Carlson (1979). None of these prescriptions, however, seem to give changes that agree with those obtained with the GCM.

To allow for the effects of cloud-height variation and lapse rate changes, we make B_1 a function of latitude and set its Legendre mode amplitudes equal to those of dF/dT shown in Fig. 2 for the GCM. These amplitudes are listed in Table 5. As indicated by the rms errors listed in the table, the Legendre polynomial series truncated at $n = 4$ fails to capture the latitudinal structure of B_1. Nevertheless, including the modes up to $n = 4$ allows for some of the latitudinal dependence. Once we have fixed the modes of B_1, we make A_1 in (4) a function of latitude and adjust it so that, given the surface temperatures of the GCM's initial state, (4) produces the appropriate IR radiative flux. The function $A_1(x)$ is then held constant. Because it remains constant, $A_1(x)$ has no direct affect on the changes calculated when the solar constant changes. Making the adjustment is necessary, however, as we would expect that the sensitivity of the EBM, like that of the GCM, is a function of the model's initial state.

Because we have made no effort to link surface temperature changes to changes in the meridional transport and emitted IR, the models adopted for these fields should not be labeled parameterizations. Such a label connotes some physical connec-

TABLE 5. Legendre mode amplitudes for $B_1(x)$.

Experiment	n	Mode amplitude (W m^{-2} °C^{-1})	rms error
+2%–(0%)	0	2.36	0.587
	2	−0.89	0.431
	4	0.33	0.417
0%–(−2%)	0	1.77	0.337
	2	−0.29	0.310
	4	−0.32	0.291
−2%–(−4%)	0	1.74	0.258
	2	−0.42	0.176
	4	0.36	0.127

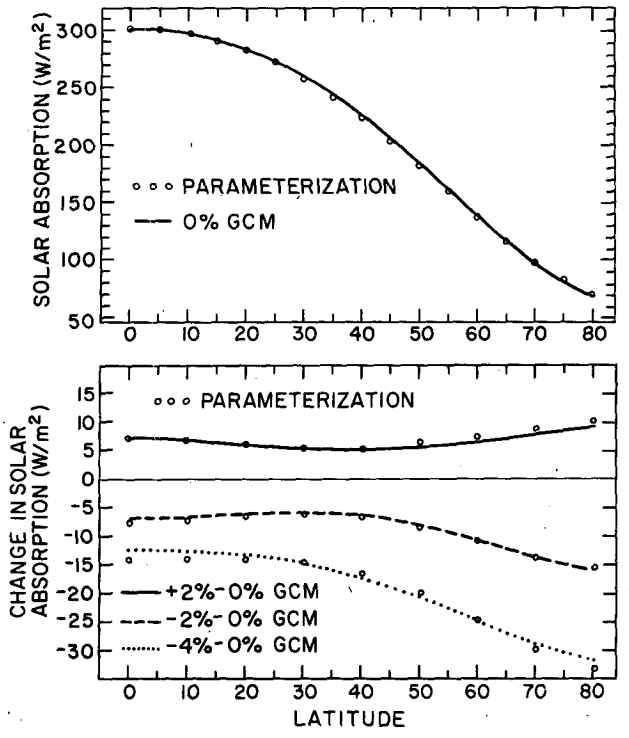

FIG. 3. Absorption of solar radiation obtained with the $n = 4$ Legendre polynomial series representation. The albedo parameterization is described in the appendix. Surface temperatures from the GCM for the four solar constant experiments constituted the input to the parameterization.

tion between the surface temperature and the energy budget component. We have only specified the changes so that they are properly correlated with changes in the GCM's surface temperature.

Unlike models adopted for the transport and emitted IR, however, a parameterization has been developed for the albedo. Such a parameterization is described in the appendix. Given the mode amplitudes of the GCM temperature fields for the four solar constant change experiments, the parameterization successfully calculates the mode amplitudes of the absorbed solar radiative flux as is shown in Fig. 3.

With these changes the EBM produces results that agree fairly well with those of the GCM as is indicated in Table 6. The large discrepancy found for the 0%–(−2%) experiment reflects the high sensitivity of the EBM to the parameterizations in this instance. By including in the EBM the changes in the divergence of the meridional transport for the 0%–(−2%) experiment ΔT_0 becomes 3.50°C. For the other solar constant changes, however, including the small transport changes has little effect on the agreement shown in Table 6. Including these changes improves the agreement only slightly.

We should remember that to achieve the agreement shown in Table 6, we relied on results from the four GCM climate change experiments to develop models for the energy budget components. To develop similar models for the earth, we would need observations of the components and the surface temperature for several distinctly different climatic states. Such observations are obviously unavailable. One wonders, however, whether we might have constructed the models by using results solely from the GCM's control experiment. For example, as is indicated in the appendix, we may have been able to derive the albedo parameterization given the procedures used to compute the absorption of solar radiation in the GCM and given the means and standard deviations of the zonal mean surface temperatures. In a similar fashion, could we have detected the feedbacks that took place in the GCM by analyzing the response of the meridional transport and IR flux to fluctuations in the model's temperature field? A provocative question for future research.

4. Conclusions

Recent studies (Cess, 1976; Lian and Cess, 1977; Coakley, 1979) have shown that with parameterizations designed to model the earth's radiation budget components, EBMs responded to changes in the solar radiative flux in much the same way as Wetherald and Manabe's GCM. Inspection of the models, however, leads us to suspect these findings. First, in the EBMs the poleward flux of heat was parameterized so that it increased as a pole-to-equator surface temperature gradient increased. For the solar constant changes under consideration the poleward flux of energy in the GCM remained relatively constant despite sizeable changes in the model's surface temperature gradient. Second, the parameterization of infrared emission used in the EBMs was designed for the earth, and it differed significantly from that obtained for the GCM. Considering these differences, we conclude that the previously reported agreement was fortuitous.

Agreement between the EBM and GCM was achieved, however, when we adopted models for the energy budget components that reproduced the changes that occurred in the GCM. These models

TABLE 6. Results for EBM with constant transport and modified albedo and IR parameterizations.

Solar constant change	ΔT_0 (°C)	$\Delta F_0/\Delta T_0$ (W m^{-2} °C^{-1})	$Q\Delta\alpha_0/\Delta T_0$ (W m^{-2} °C^{-1})
+2%–0%	2.74	2.3	−0.57
0%–(−2%)	5.99	1.6	−0.87
−2%–(−4%)	6.16	1.6	−0.91

deviated substantially from the parameterizations that were derived by following procedures normally adopted when modeling the earth's climate. By following the procedures normally used, we were unable to recover the feedbacks that governed the GCM's response to solar constant changes. We should be surprised therefore if the parameterizations similarly derived for the earth account for all of the feedbacks that could significantly affect climate change.

Acknowledgments. We gratefully acknowledge the help of Mr. R. T. Wetherald of the Geophysical Fluid Dynamics Laboratory who supplied tabulated results from the GCM experiments. We thank Dr. V. Ramanathan of NCAR who encouraged us to pursue this study and Prof. R. D. Cess of SUNY, Stony Brook, for his comments and suggestions.

APPENDIX

The Albedo Parameterization

The albedo parameterization is constructed in two steps. First, we devise a scheme that produces the planetary albedo given the corresponding surface albedo. This scheme is designed to compute the absorbed solar radiative flux in much the same way that it is computed in the GCM (Manabe and Strickler, 1964). Next we devise a scheme for computing the surface albedo given the surface temperature.

Following Manabe and Strickler (1964), we take the fraction of solar radiation absorbed to be given by

$$A = a + (1 - r - a)(1 - \alpha_3), \qquad \text{(A1)}$$

where a is the fraction absorbed by atmospheric gases, r the fraction reflected through Rayleigh scattering and α_3 the albedo of a cloudy atmosphere that is free of molecular scattering and absorption. The planetary albedo is $1 - A$. We compute α_3 by taking

$$\alpha_i = A_{c_i}\alpha_{c_i} + [t_{c_i}A_{c_i} + (1 - A_{c_i})]\alpha_{i-1}, \qquad \text{(A2)}$$

where A_{c_i} is the cloud-cover fraction for the ith level, α_{c_i} the reflectivity of the cloud, t_{c_i} its transmissivity and α_0 the surface albedo. The GCM contains three cloud levels, high, middle and low. The latitudinal distribution of cloud cover in these levels is given by Manabe (1969); the optical properties of the clouds are given by Manabe and Strickler (1964) and by Manabe and Wetherald (1975). These properties are listed in Table A1. Also, as in the GCM, $r = 0.06$.

TABLE A1. Reflectivities and transmissivities assigned to clouds.

Cloud level	i	α_{c_i}	t_{c_i}
High	3	0.200	0.795
Middle	2	0.480	0.500
Low	1	0.630	0.335

Most of the atmospheric absorption of solar radiation in the GCM is due to water vapor. The absorption changes as the concentration of water vapor changes. To allow for these changes, we assume that the relative humidity profile in the GCM remains constant. As a result, we can take the absorption to be given by

$$a = a_0 + (\partial a/\partial U)(dU/dT)(T - T_0), \qquad \text{(A3)}$$

where T and T_0 are surface temperatures and U is the column amount of water vapor. Since for typical atmospheric paths $a \propto \ln U$ and since the saturation vapor pressure $p \propto e^{-L/T}$, where L can be taken to be constant, we find that (A3) becomes

$$a = a_0 + (180/T_0^2)(T - T_0), \qquad \text{(A4)}$$

where T and T_0 are in kelvins. The constant in (A4) is derived by taking $L = 5410$ K and by taking the value of $\partial a/\partial \ln U$ from the curve given by Manabe and Wetherald (1967). Because $\partial a/\partial \ln U$ is constant over a wide range of U, and since L is constant, Eq. (A4) should be applicable over the range of humidity profiles obtained with the GCM. To reproduce the results of the control experiment it is sufficient to take $a_0 = 0.16$ independent of latitude.

Given the surface albedos, surface temperatures and cloud distributions of the GCM, Eqs. (A1), (A2) and (A4) produce good estimates of the GCM's planetary albedo at each latitude. The next step is to compute the surface albedo of the GCM given the surface temperature.

Because the ice line in the GCM is located at the −25°C isotherm and because snow falls when precipitation occurs and the temperature is 0°C just above the surface, we might expect ice and snow cover in the GCM to follow isotherms of the surface temperature. Of course, there is no well-defined ice line or snow line in the zonal average fields of the GCM as there has been in some EBMs (Budyko, 1969; North, 1975). Instead, the extent of zonal average snow and ice-cover and therefore the zonal average surface albedo varies smoothly with latitude in the GCM. This smooth variation results from the area and time averaging performed to give the zonal average features of the model. We achieve the effect of this averaging by allowing for fluctuations in the zonal mean surface temperature. We assume these fluctuations to be normally distributed so that the fraction of time the zonal average temperature T falls below a specified temperature T_0 is given by

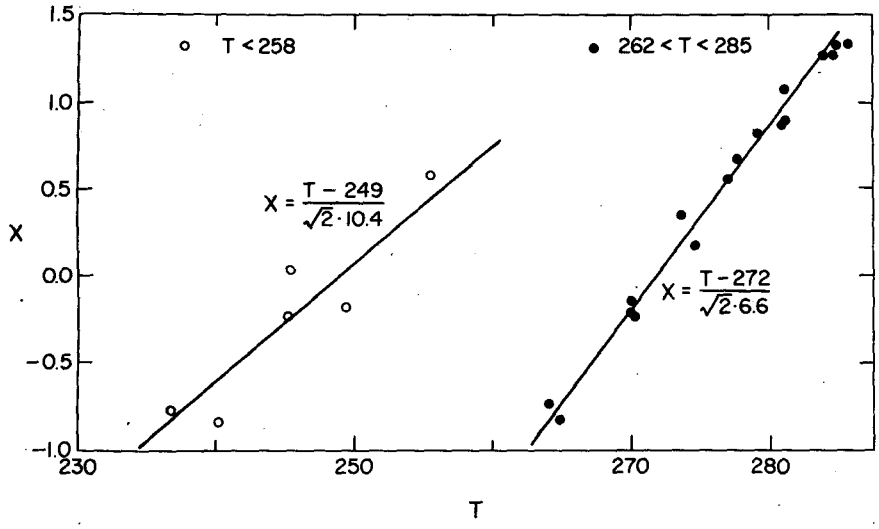

FIG. A1. $x = (T - T_0)/(\sqrt{2}\sigma)$ obtained by fitting the GCM surface albedos and surface temperatures to (A5) and (A6).

$$F(T_0,T) = \begin{cases} 1/2\left[1 + \text{erf}\left(\dfrac{T_0 - T}{\sqrt{2}\sigma}\right)\right], & T_0 > T \\ 1/2\left[1 - \text{erf}\left(\dfrac{T - T_0}{\sqrt{2}\sigma}\right)\right], & T_0 < T, \end{cases} \quad \text{(A5)}$$

where σ is the rms deviation of the zonal average temperature about its mean. The surface albedo in the GCM is then assumed to be given by

$$\alpha_0 = F_i\alpha_i + (F_s - F_i)\alpha_s + (1 - F_s)\alpha_g, \quad \text{(A6)}$$

where $F_i = F(T_i,T)$ and $F_s = F(T_s,T)$. For ice $\alpha_i = 0.70$; for snow over land $\alpha_s = 0.45$; for sea ice $\alpha_s = 0.35$ (sea ice is assumed to follow the same isotherm T_s as snow over continents); and for bare land and ocean surfaces α_g is taken to be the same as those in the GCM. Fitting (A5) and (A6) to the surface temperatures and surface albedos obtained with the GCM, we obtain, as is shown in Fig. A1, $T_i = -24$°C for the formation of ice in the GCM and $T_s = -1$°C for the formation of snow and sea ice. Because these temperatures differ little from those at which the ice edge and snow edge might be expected to exist in the GCM, the simple model of normally distributed surface temperatures appears to be realistic. Taking $\sigma = 8$°C, T_i and T_s are changed to -25 and -4°C in order to improve the fit for the Legendre modes of the absorbed solar radiative flux in the control experiment. This fit is shown in Fig. 3.

As is indicated in Fig. A1 the rms deviation of the zonal average surface temperature in the GCM appeared to range from ~7–10°C. We may speculate on the causes for this change. The larger variance was obtained for the colder temperatures. At the colder temperatures as the surface changes from being snow covered to ice covered its reflectivity jumps from 0.45 to 0.7. This jump gives a fractional change in the flux of solar radiation absorbed by the surface that is larger than the fractional change when the surface changes from being bare to being covered by snow. Because the surface temperature in the GCM is calculated from the condition of surface energy balance, the larger variance obtained for the colder temperatures reflects the larger fractional change in the solar radiation absorbed by the surface.

REFERENCES

Budyko, M. I., 1969: The effect of solar radiation variations on the climate of the earth. *Tellus*, **21**, 611–619.

Cess, R. D., 1974: Radiative transfer due to atmospheric water vapor: Global considerations of the earth's energy balance. *J. Quant. Spectros. Radiat. Transfer*, **14**, 861–871.

——, 1976: Climate change: An appraisal of atmospheric feedback mechanisms employing zonal climatology. *J. Atmos. Sci.*, **33**, 1831–1843.

Coakley, J. A., Jr., 1979: A study of climate sensitivity using a simple energy balance model. *J. Atmos. Sci.*, **36**, 260–269.

Lian, M. S., and R. D. Cess, 1977: Energy balance climate models: A reappraisal of ice-albedo feedback. *J. Atmos. Sci.*, **34**, 1058–1062.

Manabe, S., 1969: Climate and the ocean circulation: I. The atmospheric circulation and hydrology of the earth's surface. *Mon. Wea. Rev.*, **97**, 739–789.

——, and R. F. Strickler, 1964: Thermal equilibrium of the atmosphere with a convective adjustment. *J. Atmos. Sci.*, **21**, 361–385.

——, and R. T. Wetherald, 1967: Thermal equilibrium of the atmosphere with a given distribution of relative humidity. *J. Atmos. Sci.*, **24**, 241–259.

——, and ——, 1975: The effects of doubling CO_2 concentration on the climate of a general circulation model. *J. Atmos. Sci.*, **32**, 3–15.

North, G. R., 1975: Theory of energy-balance climate models. *J. Atmos. Sci.*, **32**, 2033–2043.

——, and J. A. Coakley, Jr., 1979: Differences between seasonal and mean annual energy balance model calculations of climate and climate sensitivity. *J. Atmos. Sci.*, **36**, 1189–1204.

Ramanathan, V., 1977: Interactions between ice-albedo, lapse-rate and cloud-top feedbacks: An analysis of the nonlinear response of a GCM climate model. *J. Atmos. Sci.*, **34**, 1885–1897.

——, and J. A. Coakley, Jr., 1978: Climate modeling through radiative-convective models. *Rev. Geophys. Space Phys.*, **16**, 465–489.

Rennick, M. A., 1977: The parameterization of tropospheric lapse rates in terms of surface temperature. *J. Atmos. Sci.*, **34**, 854–862.

Sellers, W. D., 1969: A climate model based on the energy balance of the earth-atmosphere system. *J. Appl. Meteor.*, **8**, 392–400.

Stone, P. H., 1978: Baroclinic adjustment. *J. Atmos. Sci.*, **35**, 561–571.

——, and J. H. Carlson, 1979: Atmospheric lapse rate regimes and their parameterization. *J. Atmos. Sci.*, **36**, 415–423.

Wetherald, R. T., and S. Manabe, 1975: The effects of changing the solar constant on the climate of a general circulation model. *J. Atmos. Sci.*, **32**, 2044–2059.